Available online at www.sciencedirect.com
ScienceDirect
C. R. Physique 8 (2007) 340–348
COMPTES RENDUS PHYSIQUE
http://france.elsevier.com/direct/COMREN/

Optical techniques for direct imaging of exoplanets/Techniques optiques pour l'imagerie directe des exoplanètes

Calibration of residual speckle in a nulling coronagraph

Michael Shao

Jet Propulsion Laboratory, California Institute of Technology, 4800, Oak Grove Drive, Pasadena, CA 91109, USA

Abstract

The most challenging aspect of the direct detection of planets around nearby stars is the huge brightness difference between planet and star associated to the very small angular separation of the two objects. This article describes the operation of a post coronagraph wavefront calibration system for measuring the residual speckle pattern, making use of the coherence of starlight. For a ground based AO coronagraph, the calibration interferometer potentially offers photon limited planet detection instead of atmospheric speckle limited detection. In a space based coronagraph, the use of the calibration system reduces the stability requirements of the optical system by several orders of magnitude. ***To cite this article: M. Shao, C. R. Physique 8 (2007).***

Résumé

Calibration des speckles résiduels d'un coronographe à compensation. L'aspect le plus compétitif de la détection directe des planètes autour d'étoiles proches est l'énorme différence de brillance entre la planète et l'étoile associée à une séparation angulaire très petite des deux objets. Cet article décrit l'utilisation d'un système de calibration du front d'onde après le coronographe pour mesurer les speckles résiduels, en utilisant la cohérence de la lumière de l'étoile. Pour un coronographe au sol utilisant une optique adaptative, cette technique permet une détection limitée par le bruit de photon et non pas par les speckles atmosphériques. Pour un coronographe dans l'espace, l'utilisation du système de calibration réduit les exigences de stabilité du système optique de plusieurs ordres de grandeur. ***Pour citer cet article : M. Shao, C. R. Physique 8 (2007).***

Keywords: Residual speckle; Nulling coronagraph

Mots-clés : Speckle résiduel ; Coronographe à compensation

1. Introduction

Over 180 planets have been detected beyond our solar system, most of them by looking at the radial velocity variations of the star caused by an orbiting planet. Astrometric detection, with ground (Keck and VLTI interferometers) and space based interferometers (SIM) will extend the discovery down to terrestrial mass planets. Recently, there has been a great deal of interest in direct detection. The two most difficult problems in direct detection is suppressing starlight by 9–10 orders of magnitude at very small angular separations; a Sun–Earth system at 10 pc would be separated by 0.1 arcsec and have a contrast of 10^{10}.

E-mail address: mshao@huey.jpl.nasa.gov.

1631-0705/$ – see front matter
doi:10.1016/j.crhy.2007.03.002

The nulling coronagraph is one of a few devices that have the potential to suppress starlight by 1e10 at 2 λ/D. An early version of a nulling coronagraph is described in Shao [1], the current design is described in Shao [2]. Suppressing the starlight to 10^{-10} is a very difficult and complex task. However, even after 1e−10 suppression, the remaining speckle pattern must be subtracted to $\sim 2 \times 10^{-11}$ or lower, in order for a 10^{-10} planet to be detected with a 5 : 1 signal/noise ratio.

This article describes the concept of a nulling coronagraph, and some of its optical properties. The main purpose, however, is to describe a post nulling coronagraph interferometer to measure the residual speckle pattern. The post coronagraph calibration interferometer can be used behind a variety of coronagraphs; a nulling coronagraph is used as example of a coronagraph that has a very small $\sim 2\ \lambda/D$ inner working angle.

In ground based AO coronagraphs, the residual speckle pattern after a long exposure will not be perfectly smooth. The dominant sources of speckle after a long exposure are called pinned speckles caused by 'non-common path' errors. The term non-common path error refers to the fact that the wavefront sensor for the AO system does not measure all the wavefront errors seen by the coronagraph and camera. Pinned speckles can be as bright as a few times 10^{-4} of the star.

One can very roughly estimate the atmospheric non-uniformity of a ∼1 h integration. If a ground based AO system (@1.6 μm) can achieve a 95% strehl, with ∼4000 actuators, the speckle pattern will have a flux level ∼0.05/4000 ∼1.2e−5 below the stellar image. If the speckle lifetime, after the AO coronagraph, is ∼0.5 s, then after an hour, the speckle pattern should be smooth to $\sim 1.5 \times 10^{-7}$.

In contrast, if we could directly measure the residual speckle pattern, without the planet, the photon limited 'smoothness' of the speckle pattern is ∼3e−9. The approach described in this paper. The measurement of the residual PSF is made on a time scale faster than the atmospheric speckle change timescale and, in theory, should accurately represent both instrumental and atmospheric speckles.

Direct measurement of the residual speckle pattern is equally important for a space based coronagraph. Several techniques for doing this have been investigated. One approach requires the speckle pattern to be stable while the telescope rotates about the line of sight. Another makes use of the radial streaking of speckles with wavelength. The technique described here is based on the coherence of starlight (the non-coherence with planet light).

Direct measurement of the speckle pattern is concurrent with recording of the science image, and hence relaxes the wavefront stability of a space based telescope and coronagraph/nuller by many orders of magnitude.

2. Nulling coronagraph and calibration interferometer

The nulling coronagraph is a coronagraph, based on a nulling interferometer, as opposed to more familiar designs of an apodized aperture telescope, and Lyot coronagraph. Like Lyot coronagraphs, the nulling coronagraph is not a single design but a family of designs. We describe one version of the nuller, for illustrative purposes, and compare its properties with more conventional apodized aperture telescopes, and Lyot coronagraphs.

2.1. From Nulling interferometer to nulling coronagraph

Nulling interferometers were originally designed to work in the thermal IR range, with multi-telescope interferometers. At a wavelength of 10 μm, baselines of several 10s of meters were needed to resolve a star from a planet 0.1 arcsec away. As we go to shorter wavelengths, the required baseline gets shorter, linearly with wavelength. At visible wavelengths, the needed baseline, ∼1 m, was significantly smaller than the size of the telescope needed to detect a 30 mag planet. The nulling interferometer design had to be turned inside out.

The nulling interferometer had one very attractive feature, and one significantly unattractive feature. Nulling interferometers were designed to totally suppress starlight on axis, but at an angle of only $\lambda/2B$, where B is the interferometer baseline, let the planet light through the system. An unattractive aspect of an IR interferometer was the need to rotate the baseline around the line of sight (to fill the UV plane) before a synthetic image could be generated. The visible nuller retains the advantage of a nulling interferometer of being able to suppress starlight while letting planet light through at 1–2 λ/D, and the convenience of a filled aperture coronagraph of forming a direct image of the sky without need for rotational synthesis, Shao [1].

A conceptual drawing of a nulling coronagraph is show in Fig. 1. A more detailed description of its operation is given later.

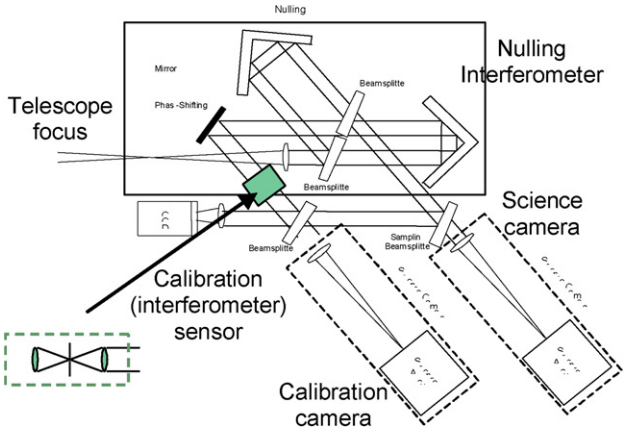

Fig. 1. Concept for a calibration wavefront sensor with a nulling coronagraph.

2.2. *The importance of a small inner working angle.*

Planets around nearby stars can be directly detected either by its reflected light, or its thermally emitted light. At visible and near IR wavelengths, only very young planets will have significant emitted flux. For mature planets, the Vis/NIR flux is reflected starlight. For reflected light, the closer a planet is to the star, the brighter it is. A Jupiter at 5 AU is 1e−9 of the brightness of its parent star. At 1 AU, it's 25 times brighter. In searching for Earths in the habitable zone, the size of the inner working angle is even more important. For a Sun like star the habitable zone is roughly at a radius of 0.7–1.4 AU. The angular separation of an Earth–Sun at 10 pc is only 0.1 arcsec. There are only ∼40 FGK single stars whose habitable zone is larger than 0.1 arcsec. Reducing the inner working angle by 2×, will increase the number of potential targets by almost an order of magnitude.

2.3. *Overview of a nulling coronagraph*

In analogy to Lyot coronagraphs, nulling coronagraphs are a class of instruments as opposed to a single design. The basic idea is shown in Fig. 1. Light from a telescope enters a Machzender type interferometer, but is recombined with a π phase shift, and a pupil shear. The π phase shift results in an interferometric null, and the shear means only light coming on-axis will see the π phase shift.

In this simplified version of a nulling coronagraph, if the two arms have exactly equal optical path, the output will be constructive interference, instead of the desired destructive interference. A π phase shift is obtained by changing the delay in 1 arm of the interferometer. For a fixed delay, the phase shift is dependent on the wavelength of the light and an exact π phase shift is obtained only at one wavelength. To broaden the wavelength range over which a deep null is obtained, we place slightly more glass in one arm of the interferometer. The dispersion of the glass combined with the inserted delay in vacuum gives rise to a broad band deep null. One design of an achromatic nuller using fused silica and BK7 glass is shown in Fig. 2. Experimental demonstration of a deep null would not be fundamentally limited by dispersion.

2.3.1. *Wavefront sensing and control in a nulling coronagraph*

In the coronagraph of Fig. 1, the output will have no light if the two interfering beams have a π phase shift and equal intensity. The nulling interferometer at its output divides the pupil into ∼1000 sub apertures, with a lenslet array. The lenslet array focuses the light in each sub aperture into a single mode fiber. Perfect starlight suppression is achieved if the amplitudes in the fiber from the two arms are exactly equal and the phase difference is π. The sensitivity to slight mismatches in intensity and phase are given by the following equation:

$$\text{Stellar leakage} = (dI/I)^2/16 + (d_\phi)^2/4$$

where dI/I is the fractional difference in the intensity of the two beams, and d_ϕ is the phase error in radians.

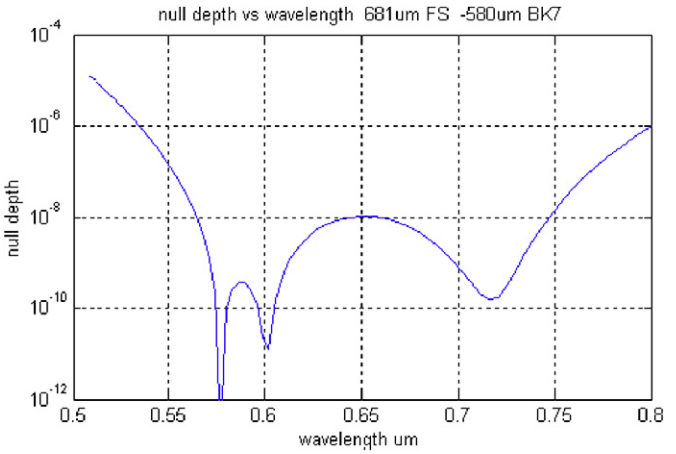

Fig. 2. Characteristics of an achromatic nuller.

The light at the output of the array of single mode fibers is re-imaged onto a CCD detector. Intensity balance of the two arms is measured by placing a shutter in one arm of the nuller at a time. Phase is measured by dithering the optical path around null.

The accuracy in measuring dI/I and d_ϕ are ultimately limited by photon statistics:

$$\sigma(dI/I) = 2 \times \sqrt{N} \quad \text{and} \quad \sigma(d_\phi) = \sqrt{2}/\sqrt{N}$$

where N is the number of photons detected during the measurement.

In the measurement approach described here dI/I is measured sequentially with d_ϕ—the two are not measured at the same time.

When dithering around a deep null the fraction of photons blocked by the nuller is very near unity. At this point other sources of noise like the CCD dark current, local and exozodi and CCD read noise may dominate over photon noise. These other sources of noise can be significantly reduced with the calibration interferometer described in the next section, leaving the system limited only by photon noise from the star.

3. Overview of the calibration interferometer

A nulling coronagraph has two optical outputs, the dark output is where the light has been removed so the planet can be detected, and the bright output where 99.999+% of the starlight is directed.

The calibration interferometer takes part of the dark output and interferes it with a spatially filtered wavefront from the bright output, as seen in Fig. 1. The calibration interferometer is path length dithered so that the outputs can be demodulated to measure the amplitude and phase of the wavefront in the 'dark' output of the coronagraph.

The electric field of the dark output has two uses: one is to feed back to the wavefront and control system to reduce the scattered light in the dark output of the coronagraph, and the second is to use the E field to estimate the residual speckle pattern in the science camera.

This concept is similar to the SISS (Guyon [3]), where a spatially filtered flat 'reference' beam is interfered with a 'converging' beam from the dark output of the coronagraph. There are actually 4 variants. The 'reference' beam can be a plane wave or a converging spherical wave, and the 'dark' beam can be a plane wave or a converging beam. If the gross wavefront of the two interfering beams are different, e.g. a converging spherical wave and a plane wave, the resulting interference is inherently narrow band because the optical path at the edge of the pupil is grossly unmatched. That eliminates two of the 4 options. Of the two remaining options, combining two converging beams or two plane waves are fundamentally the same. However, if a bright 'ref' beam is combined with the faint output of a coronagraph and detected at an image plane, the bright 'ref' beam will produce a very bright airy spot which will greatly increase the needed dynamic range of the detector. As a result, we chose to interfere two plane waves and do the detection in the pupil plane.

3.1. Calibration interferometer and heterodyne advantage

In Section 2.3.1, the wavefront sensing for a nulling coronagraph was briefly described. In measuring the intensity difference in the two arms of the nulling interferometer, one arm at a time is blocked. In measuring the phase difference, the optical path in one arm of the nuller is changed by a small amount. If the nuller is working in the visible (550 nm), a pathlength difference in the two arms of 0.1 nanometers means the light leakage is 3e−7.

Deformable mirrors (DM) can be moved with very high resolution, sub-angstrom. However, they are not accurate to 1 part in 10 000. Electrostatic DMs, piezoelectric and electrostrictive DMs have significant nonlinearities that make it impossible to move large distances (e.g. 1 μ) with angstrom accuracy. Small motions, a few nanometers, can be commanded with sub angstrom accuracy. As a result, when dithering to find the optical path for the best null, it's best not to move the DM too far from null.

A 5 mag G star at 10 pc would produce ∼4e8 photons/s into a 2 m telescope. In a nulling coronagraph with a ∼1000 element DM, each channel would have ∼400 000 photons/s. However, if we are very close to null, say a null of 1e−7, the photon flux would be 0.045 photons/s. If the imaging field of view was 10 square arcsec, and we were looking out of the local zodi 45 deg from the ecliptic pole and the target star's 1 zodi disk was also viewed at an angle of 45 deg, the combination of local/exo-zodi would produce ∼3 photons/s, ∼65 times the brightness of residual starlight.

Zodi background, CCD dark current, CCD readnoise are noise sources that dwarf the photon noise from the star. However, by interfering this very faint light with the light from the bright output of the nuller, the interference signal is boosted. If the bright arm of the calibration interferometer is on average a million times brighter than the dark arm, the average fringe visibility is given by

$$\text{vis} = 2 \times \sqrt{}(I1 \times I2)/(I1 + I2) \sim 0.002 \quad \text{when } I2 = 1e6 * I1$$

The fringe signal would be 500 times fainter the light in the bright arm but 2000 times brighter than the light in the dark arm. So while the signal has grown, the noise has also grown by a factor $\sqrt{}(I2 + I1)/\sqrt{}(I1)$ if the system is photon limited. However, the larger signal means that other noise sources such as local and exo-zodi, ccd read noise and dark current, are less important by a factor of $\sqrt{}$(intensity ratio). For a 1e6 intensity ratio we are now 1000 times more tolerant of zodi background for wavefront sensing.

3.2. Calibration interferometer and PSF subtraction

Most coronagraphs hope to achieve star light suppression at a level where the residual scattered starlight has the same flux (photons/sq arcsec) as the planet, the so-called $Q = 1$ condition. However, even when the residual starlight is equal to that of the planet, we need to, in the post-detection process, reduce the fluctuations in the scattered light background to a level that is 5 to 10 times lower than the planet flux to detect the planet with a SNR of 5–10.

3.3. PSF subtraction for space coronagraphs

Many approaches have been suggested for PSF subtraction; some approaches only work for a space based telescope, whereas others are designed for used with ground based extreme AO coronagraph systems. The approach here can be used in space or on the ground.

Many telescopes in space can be rotated about the line of sight. The main requirement is that the residual speckle pattern, the PSF, be stable to ∼0.1 the planet flux during the whole duration of the measurement. The time scale for this type of PSF subtraction is typically 2–3 h. This technique can be used on ground based telescopes and is called angular differential imaging (Marois [8]). A 1 h observation followed by a 1/2 to 1 h 'roll' maneuver and another 1 h observation. For the detection of terrestrial planets 1e−10 contrast, stability to 1e−11, the wavefront of the telescope and subsequent optics has to be stable to a few (<10) picometers over a several hour time frame.

If the telescope primary and secondary distances change by a nanometer, the wavefront can pick up many 10s of picometers of focus error. Coronagraphs that have a small inner working angle, e.g. $2\,\lambda/D$, are much more susceptible to focus and other low order wavefront errors than coronagraphs with a larger, say $4\,\lambda/D$, inner working angle. This very tight wavefront stability requirement drives almost every aspect of a space telescope/coronagraph design.

The calibration interferometer offers a way to avoid this very tight wavefront stability requirement in space based systems. When a coronagraph images the region around a star and the residual light level is 1×10^{-10} of the star, the

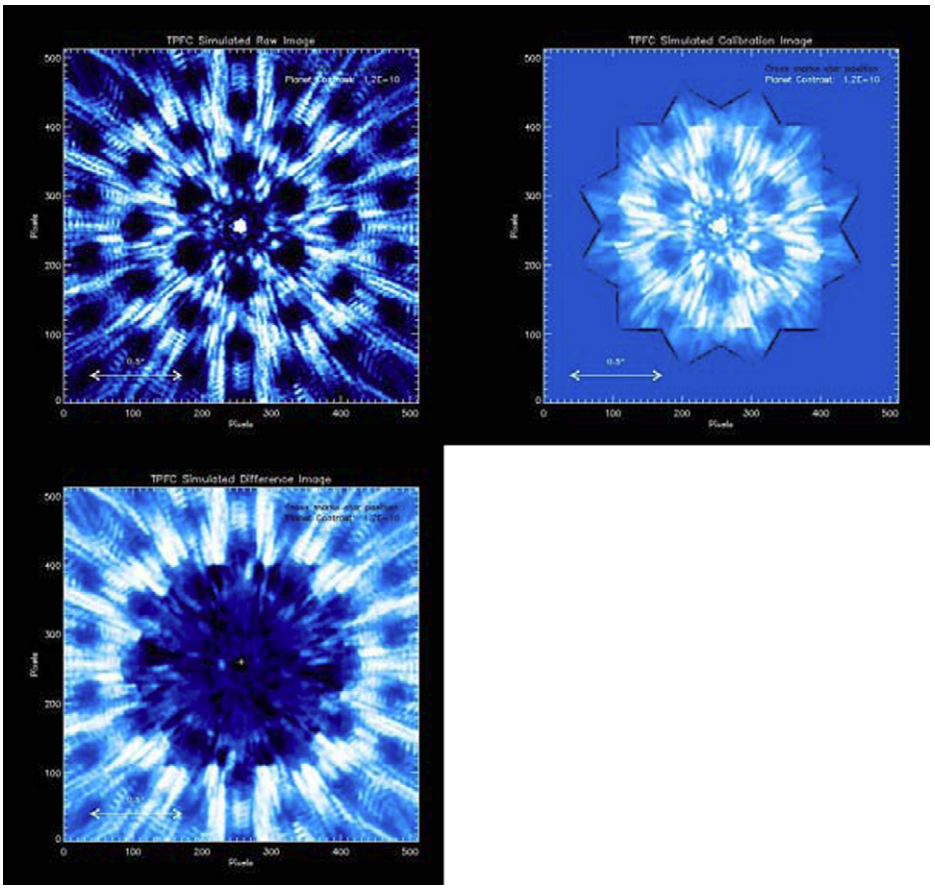

Fig. 3. A simulated image of an Earth-like planet at 10 pc taken through the 8 × 3.5 m aperture TPF telescope. Top left, raw image after 3 1-h exposures taken 120 degrees apart. Top right, estimate of leaked starlight psf. Bottom left, psf subtracted image.

implication is that half of the field of view is brighter than 10^{-10} and the other half dimmer. Typically, the field is small, a few arcsec in diameter, but an average flux of 10^{-10} implies that there could be several hundred speckles as bright as an Earth-like planet. Only one of those speckles is a planet.

Our technique makes use of the coherence of starlight, that is, light from the star is coherent (will interfere coherently) with speckles whose origin is scattered starlight, but will not interfere with light in the focal plane that comes from the planet (or dust) orbiting the star.

The calibration interferometer measures the electric field of the light at the dark output of the coronagraph. The square of the Fourier transform of that electric field is the PSF of the system. The elimination of the stability requirement arises because we make this PSF measurement simultaneously with the science image. If the PSF measurement is simultaneous with the science measurement to 3 milliseconds, then the 10 picometer/3 h stability requirement becomes 10 picometer/3 ms—it has been relaxed by a factor of a million.

Fig. 3 shows a numerical simulation of PSF subtraction as will be used in a terrestrial planet finder coronagraph instrument. The simulation by B. Lane shows the raw PSF of a nulling coronagraph (3 azimuth rotations to cover the whole sky) and the reduction of the speckle artifacts after PSF subtraction (Shao [3]).

The removal of this picometer stability requirement has other implications. The first is that we can now seriously think about coronagraphs working at 1–2 λ/D instead of 4–5 λ/D, since, otherwise, it would have been impossible to meet the wavefront stability requirement. Another consequence of using the calibration interferometer for PSF estimation is that one no longer needs to rotate the telescope about the line of sight, thus saving observing time. However, a several orders of magnitude relaxation in stability also means a simpler, less demanding thermal control subsystem, from a few 10s of microK to perhaps 10s of milliK.

3.4. PSF subtraction for ground coronagraphs

For ground based AO coronagraphs, the situation is a little different. The atmosphere is a major impediment to high contrast imaging. In space it is, in theory, possible to suppress the starlight by 1×10^{-7} so that at 3 λ/D the scattered starlight's surface brightness is 1e−10 of the stellar image. On the ground, an extreme AO system that gets 95% strehl with a ∼2000 actuator deformable mirror would have a 'halo' with a surface brightness of 2.5×10^{-5} of the star, a factor of 10^5 higher than what is theoretically possible in space. Ground based coronagraphs depend on two techniques: averaging of the speckles in the halo, and PSF subtraction.

If the speckles in the image plane have a lifetime of ∼1/3 s, then after 1 h, the bumpiness of the halo will be reduced by $\sqrt{}(3600 \times 3) \sim 100$ below the $\sim 2.5 \times 10^{-5}$ level to $\sim 2 \times 10^{-7}$ (Sivaramakrishnan et al. [4]).

If ground based coronagraphs are to have any hope of detecting mature (several GYr old) Jovian planets, PSF subtraction is an absolute necessity. Four approaches for PSF subtraction have been studied, the last one being the use of the post coronagraph calibration interferometer. The potential and limitations of the 4 approaches are discussed.

One approach to PSF subtraction makes use of the fact that many Jovian planets have a strong methane feature (Racine [5]). Three images are recorded, in the methane band and either side of the methane band. Detection cannot use all of the available light because the speckle pattern changes with wavelength, so only a narrow part of the spectrum around methane can be used.

A second approach makes use of the radial spreading of the speckle pattern at longer wavelengths (Sparks [6]). This approach only works at relative large angular separations $>5\ \lambda/D$, because over a 20% bandpass the radial spread of the speckles is only 20%. In addition, the speckles spread radially only for phase and amplitude errors in the pupil. In most coronagraphs, there are many optical elements not at a pupil, and wavefront errors from these elements would not have the same radial spread relation as errors in the pupil.

A third approach takes two simultaneous images in orthogonal polarizations. If the target is polarized, such as a circumstellar disk of dust, the image in one polarization can be used as an estimate of the PSF of the telescope/coronagraph.

The forth approach, described in this article, identifies which speckles are 'scattered starlight' by interfering the post coronagraph light with a 'reference' beam of starlight. By measuring the electric field (phase and amplitude) at the output of the coronagraph, on a time scale faster than the atmospheric time scale, this approach will capture both slowly varying instrumental speckles as well as the residual fluctuations in the halo after averaging the atmosphere for an hour.

While PSF subtraction is the final application of the post coronagraph interferometer, the first application is to measure the wavefront errors that create 'pinned speckles' in a ground based AO coronagraph. In any AO coronagraph the AO wavefront sensor measures the wavefront as it exits the AO system, it does not measure the wavefront at the coronagraph. In addition, all AO coronagraphs use visible light wavefront sensors for the AO system and the systematic difference between the visible wavefront and the near IR science camera gives rise to additional 'non-common path' errors. These non-common path errors also change slowly with time, especially in cass-mounted instruments where the gravity vector is changing with time and the alignment of the AO system and coronagraph slightly change with both temperature and gravity vector (Aime and Soummer [7]).

In summary the post coronagraph interferometer is designed to in real time, eliminate 'pinned speckles' due to non-common path wavefront errors, then in post processing allow PSF subtraction that makes no assumptions as the nature of the target (e.g. polarized or has a strong spectral feature) nor that wavefront errors originate at a pupil. Table 1 summarizes the potential performance of a ∼3000 actuator AO coronagraph using the post coronagraph interferometer.

3.5. Limitations and approximations

The calibration interferometer measures the E field of the output of the coronagraph and from that, estimates the speckle pattern. Several effects can bias the measurement of the E field. The first is spatial sampling. The detector that measures the interference between the 'reference' beam and the coronagraph output has a finite spatial resolution. If the coronagraph output has a high spatial frequency content, the fringe visibility will be suppressed, and, in addition, some of the high frequency error can alias down to lower spatial frequencies. This is a common problem in AO

Table 1
Potential performance of a ∼3000 actuator AO coronagraph using the post coronagraph interferometer

Optical Suppression			
effect	mitigation	residual light	w/o mitigation
Atmos	AO (~2000 actuators 95% strehl)	~$1x10^{-7}$	~1
Diffraction sidelobes	Coronagraph	< $1x10^{-9}$	~$1x10^{-3}$
Pinned speckles	Calib Interferometer	<$1x10^{-7}$	~$1x10^{-4}$
Total optical contrast		~$1x10^{-7}$	
PSF subtraction (post processing)			
Technique	hardware needed	Possible improvement	Caveats
Angular Diff Imaging	rotate telescope about line of sight	10~30	Speckles need to be stable over rotation
Diff Spectral Imaging	DSI camera or IFS	10~30	target has strong spectral signature
Radial speckle spread	IFS Integral field spectrograph	5~20	> 5λ/D and wavefront errors at a pupil
Diff Polarization imaging	polarizer	~100x	target is polarized
Stellar coherence	Calib Interferometer	~30 for 25% bw	

wavefront sensors and a reasonably good solution is to optically spatially filter the output of the coronagraph before the light reaches the interferometer.

A second possible bias is temporal smearing. The calibration interferometer should make measurements as quickly as possible to capture time varying speckles. If the electric field at the output of the coronagraph is $E(t)$, the speckles are the square of the FFT(E). This square operation is non-linear so $\text{FFT}(\langle E(t)\rangle)^2$ is not equal to $\langle \text{FFT}(E(t))\rangle^2$. Under most circumstances, high spatial frequency fluctuations will evolve more rapidly in time, and, as a result, speckle far from the center will not be as well estimated. Fortunately, the area closest to the star will be accurately estimated and that part of the field of view is why we have a coronagraph in the first place.

The last term is spectral. The calibration interferometer will measure the E field averaged over a range of wavelengths. Again, if the wavefront in the pupil plane changes a lot over the 20–25% bandwidth of the detector, there will be an error in the estimated PSF. We have conducted numerical simulations of this effect and the results are that over a ∼25% bandwidth, the error in the reconstructed PSF is ∼3%.

4. Projects using the post coronagraph calibration interferometer

At present the post coronagraph calibration interferometer is planned to be used in:

- PICTURE: A nulling coronagraph on a sounding rocket;
- GPI: Gemini Planet Imager (an AO coronagraph for the Gemini Telescope).

The post coronagraph calibration interferometer is also part of studies for future coronagraph projects:

- TPF-C: One of 3 coronagraph instrument studies funded by NASA;
- TMT EXAOC: An extreme AO coronagraph for the TMT telescope;
- Proj 1640: A collaboration between AMNH, Caltech and JPL for an extreme AO coronagraph on the Palomar 5 m telescope;
- Future balloon borne coronagraphic telescope.

In space based coronagraphs, the use of a post coronagraph calibration interferometer for PSF estimation can reduce the wavefront stability requirements of the telescope and coronagraph by many orders of magnitude. On ground based extreme AO coronagraphs, the post coronagraph calibration interferometer performs both the job of removing 'pinned speckles' by measuring the non-common path wavefront errors at the output of the coronagraph, in the science waveband, as well as provide a means for PSF subtraction that does not place restrictions on the target, such as the presence of a strong spectral or polarization feature.

Acknowledgements

This work was performed at the Jet Propulsion Laboratory, California Institute of Technology, under contract to the National Aeronautics and Space Administration.

References

[1] M. Shao, Hubble extra-solar planet interferometer, SPIE 1494 (1991).
[2] M. Shao, et al., A nulling coronagraph for TPF-C, in: J.C. Mather, et al. (Eds.), Space Telescopes and Instrumentation I: Optical, Infrared, and Millimeter, in: Proceedings of the SPIE, vol. 6265, 2006, p. 626517.
[3] O. Guyon, Astrophys. J. 615 (2004) 562.
[4] A. Sivaramakrishnan, J.P. Lloyd, P.E. Hodge, B.A. Macintosh, Speckle decorrelation and dynamic range in speckle noise-limited imaging, Astrophys. J. Lett. 581 (1) (2002) L59–L62.
[5] R. Racine, G.A.H. Walker, D. Nadeau, R. Doyon, C. Marois, Speckle noise and the detection of faint companions, Publ. Astron. Soc. Pacific 111 (1999) 587–594.
[6] W.B. Sparks, H.C. Ford, Astrophys. J. 578 (2002) 543.
[7] C. Aime, R. Soummer, The usefulness and limits of coronagraphy in the presence of pinned speckles, Astrophys. J. Lett. 612 (2004) L85.
[8] C. Marois, D. Lafrenière, R. Dovon, B. Macintosh, D. Nadeau, Angular Differential Imaging: A powerful high-contrast imaging technique, Astrophys. J. 641 (2006) 556–564.